Electro-Hydraulic Variable-Speed Drive Network Technology– First Experimental Validation

Lasse Schmidt * and Mikkel van Binsbergen-Galán

Posted Date: 13 May 2024

doi: 10.20944/preprints202405.0807.v1

Keywords: Electro-hydraulic Variable-speed Drive Networks; Electro-hydraulic Cylinder Drives; Energy Efficiency; Power Sharing; Hydraulic Actuation; Linear Actuation

 doi:10.20944/preprints202405.0807.v1

Article

Electro-Hydraulic Variable-Speed Drive Network Technology – First Experimental Validation

Lasse Schmidt * and Mikkel van Binsbergen-Galán

AAU Energy, Aalborg University, Pontoppidanstraede 111, 9220 Aalborg, Denmark; lsc@energy.aau.dk
* Correspondence: lsc@energy.aau.dk; Tel.: +45-2232-2622

Abstract: The improvement of energy efficiency of hydraulic systems remains to be an essential challenge for the industry, and the demand for more sustainable solutions is increasing. A main focus in this endeavor is the ability to eliminate or strongly reduce the use of throttle control valves which have been the preferred control element in industrial hydraulic systems for decades. Components have been subject to continuous evolution, and current industrial grade hydraulic pumps and motors are both efficient and reliable. Even though few percentages of energy efficiency can still be achieved, the main achievements in terms of efficiency is associated with novel system designs rather than further development of components. An area subject to increasing attention is the field of variable-speed displacement control, allowing to avoid the main control valve throttle losses. Systems using this technology are, however, mainly developed as standalone drive systems, necessitating maximum force, speed and power installed in each axis, with limited hydraulic power distribution capability as compared to valve controlled systems. An emerging field addressing this challenge is so-called electro-hydraulic variable-speed drive networks which allow to completely eliminate the use of control valves and enables power sharing both electrically and hydraulically, potentially reducing the necessary installed power in many cases. The idea of such a technology was first proposed in 2022, and so far developments reported in literature have mainly been of theoretical nature. This article presents the first ever experimental results for a dual cylinder electro-hydraulic variable-speed drive network prototype. The prototype has been developed for an industrial application, but has initially been implemented in a laboratory testbench. Extensive data acquisition has been conducted while subject to the associated industrial motion cycle, under different load conditions. The data is further used in combination with models to predict the total efficiency of the drive network prototype under higher loads than what could be achieved in the laboratory, suggesting a total efficiency from the electric supply to the cylinder pistons of 68 %. Re-configuring the prototype to a known standalone drive system structure implies comparable efficiencies. Finally, the drive network is theoretically compared to a valve drive solution, generally suggesting the prototype drive network to provide efficiency improvements of at least 40 % in comparison.

Keywords: electro-hydraulic variable-speed drive networks; Electro-hydraulic Cylinder Drives; energy efficiency; power sharing; Hydraulic Actuation; Linear Actuation

1. Introduction

Throttle control valves has been the preferred control elements in hydraulic systems for decades. However, facing the current climate crisis, the high losses associated with this control approach poses a serious challenge for the industry. Hence, efforts to develop more efficient hydraulic drive technologies are increasing. Here, digital hydraulic displacement and flow control as well as variable-speed electro-hydraulic displacement control have been main focus areas.

The success of digital hydraulic technology is dependent on the successful development of new components, especially sufficiently fast switching valves [1–3], and have been reported successfully applied in different applications [4–11]. Despite these efforts which have been ongoing for nearly four decades, this technology has yet to make a broad breakthrough in industry. The reason may be associated with the inherent flow switching that may challenge system controllability and performance, besides the use of non-mass produced components that may cause the technology to be cost intensive compared to alternative approaches. A more recent contribution in this field is a so-called digital

 doi:10.20944/preprints202405.0807.v1

hydraulic oscillation transformer [12] subject to fewer and more simple components, potentially allowing to overcome these challenges. However, this technology is still at an early stage in its development.

Where digital hydraulic technology relies on switching valves with special features not necessarily available in industry, variable-speed electro-hydraulic displacement control technology mainly relies on well known components in terms of electric motors, inverters and hydraulic pumps and/or motors, realizing so-called variable-speed displacement units (VsD's). The main challenges in this area is how to design hydraulic systems whiteout the use of throttle valves while achieving the desired functionalities for specific applications. The technology has mainly evolved as single cylinder drives i.e., standalone drives, and several solutions have been reported in literature e.g., with single electric motor/single displacement units [13–15] including tandem displacement unit solutions [16,17] as well as solutions comprising two electric motors and two displacement units [18,19]. Also, drive solutions incorporating regenerative capabilities have been reported [20–22]. While these solutions are developed as single axis drives, attention to multi-axis solutions is more limited in literature. This field is however under development, and comprises e.g. VsD's combined with directional valves [23–26]. Also, the field of electro-hydraulic variable-speed drive networks is emerging after its first introduction in 2022 [27]. Since then, developments have focused on their control, component downsizing perspectives, design foundation in terms of load cycles and application in construction machinery [28–31]. These drive networks are constructed from a number of VsD's connected to cylinder chambers in a *meaningful* way and potentially with the use of chamber short-circuits, effectively reducing the number of control volumes. These features enable electro-hydraulic power sharing that may lead to a reduced number of VsD's compared to standalone type solutions, as well as potential downsizing's of the associated power installations, dependent on the load requirements of the machine. So far, findings in this area have been of theoretical nature.

This article presents the first experimental validation of electro-hydraulic variable-speed drive network technology ever conducted. These are acquired from the first electro-hydraulic variable-speed drive network prototype ever realized, produced for actuation of a so-called industrial *moving floor* application comprising two cylinders. The prototype has been implemented in a laboratory testbench made for the specific purpose of validating the basic functionality of the drive network prototype. The cylinders of the industrial application are rather large and able to produce rather high forces, while the possibility to apply loads under laboratory conditions have been limited. For this reason, the prototype laboratory validation only encompass part load operation while the motion pattern and cycle frequency of the industrial application are maintained. Hence, besides validating the prototype experimentally, the efficiency properties under higher loads are predicted using data aided model based analyses and furthermore compared to a standalone electro-hydraulic drive solution. Finally, the prototype is compared to a conventional valve control solution.

2. Dual Cylinder Electro-Hydraulic Variable-Speed Drive Network Testbench

The dual cylinder electro-hydraulic variable-speed drive network (EDN) testbench is shown in Figure 1, where the upper part depicts the functional schematics of the testbench and the lower part shows a picture of the physical testbench. The testbench comprises two cylinders with a short circuit of the piston side cylinder chambers, ideally resulting in three control volumes which may be controlled by three (pairs of) VsD's. As mentioned above, the EDN has been developed for a moving floor application, allowing this to be demonstrated in an industrial environment. The moving floor application is subject to large cylinders and motion cycle frequencies up to 16 cycles/minute, resulting in high flow requirements for the drive system. Hence, to realize the functionality with standard electric drives, each VsD function is realized as a pair of identical VsD's, i.e. there are six VsD's with these operated as three. The VsD's connected to the hydraulic tank are denoted *supply units* (SU1 and SU2) while the VsD's that are connected between cylinder chambers are denoted *drive units* (DU1.1, DU1.2, DU2.1 and DU2.2) as depicted in Figure 1. Hence, when operated in pairs this means that drive

Preprints.org (www.preprints.org) | NOT PEER-REVIEWED | Posted: 13 May 2024 doi:10.20944/preprints202405.0807.v1

units DU1.1, and DU1.2 are subject to the same speed command and similarly with DU2.1, DU2.2 and SU1, SU2.

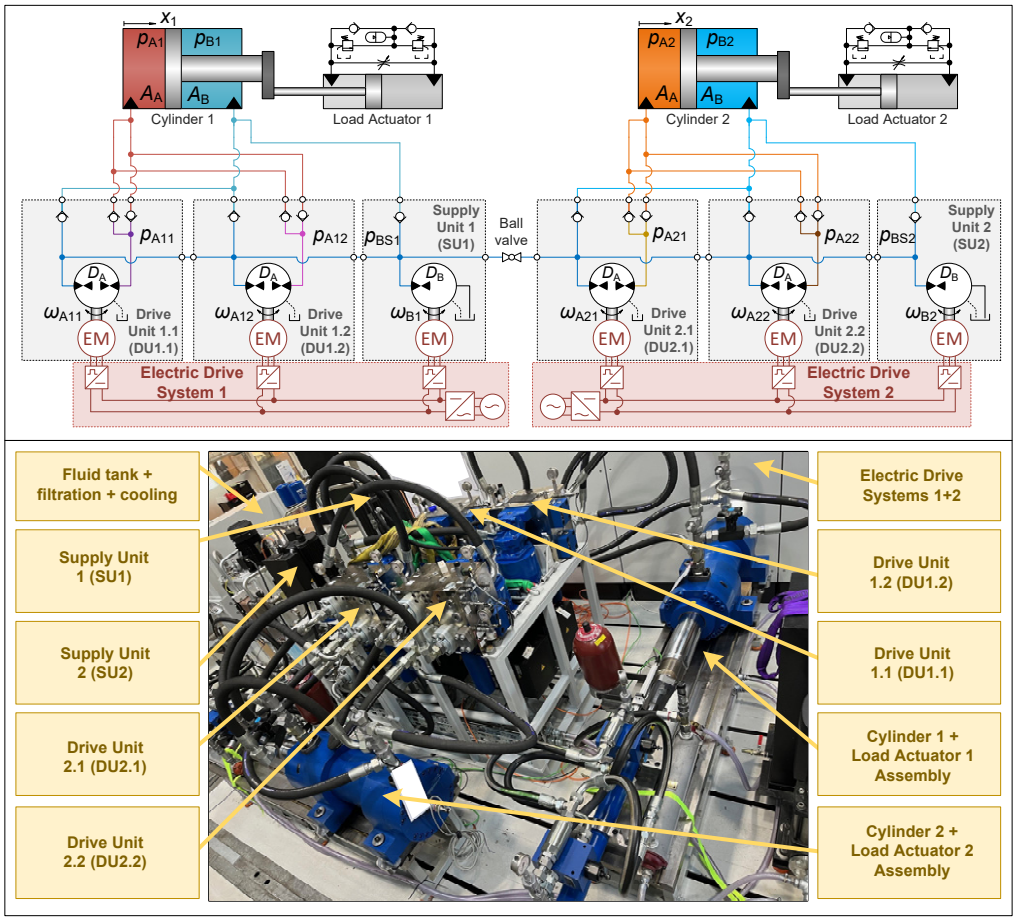

Figure 1. Functional schematics and physical laboratory testbench illustration of dual cylinder electro-hydraulic variable-speed drive network prototype.

The industrial moving floor application is subject to lengthy fluid lines between the EDN and the cylinders. Hence, to ensure a reasonable level of fluid filtration and cooling at the fluid tank level, a fluid exchange mechanism has been realized comprising parallel lines between the EDN and the cylinders, with check valve functions ensuring separate flow paths to and from the cylinders and the EDN. This functionality increases the transmission losses compared to standard fluid lines, but prevents excessive heating of the fluid.

For laboratory tests and functional validation, the load forces are realized by *passive* load actuators with limited force capability, established via pressure reduction valves. This is not an ideal load mechanism for two main reasons: 1) The inertia masses are rather low, and with the back-to-back mechanically coupled cylinder/load actuators, the eigenfrequencies of these assemblies become high relative to the industrial moving floor application. 2) The cylinders of the load actuators have substantially smaller diameters compared to the *main* cylinders (see Table 1), hence only limited load forces can be applied to the main cylinders. However, the test setup does allow to validate the basic controllability of the EDN, the main transmission losses under part load, etc., rendering the test bench feasible for experimental validation of the basic technology. Finally, the main components used in the testbench are listed in Table 1.

 doi:10.20944/preprints202405.0807.v1

Table 1. Main components of dual cylinder electro-hydraulic- variable-speed drive network testbench drive. [a]Bosch Rexroth AG, [b]Balluff GmbH.

Configuration	Description	Pcs.
[a]A2FMM125/70	Hydralic bent axis motor used in Drive Units	4
[a]PGH5-3X/100	External gear pump used in Supply Units	2
[a]LC40A10E7X/	Logic cartridge valves (check valve functions)	2
[a]HM 20-2X/	Pressure sensor (various ranges)	8
[b]BTL7-V50E-M1000-P-C003	Position sensor (etherCAT)	2
[a]Cylinder: 220/140-400 [mm]	Cylinder 1 and 2	2
[a]Cylinder: 80/56-770 [mm]	Cylinder of load actuator 1 and 2	2
[a]MS2N13-E1BHL-CSEG0	Electric motor used in Drive and Supply Units	6
[a]ctrlX XVR2-W0072ARN	Electric power supply	2
[a]ctrlX XMS2-W0250ANN	Electric inverter drive used in Drive Units	4
[a]ctrlX XMS2-W0210ANN	Electric inverter drive used in Supply Units	2
[a]ctrlX Core	Control hardware for control software implementation	1

3. Experimental Results, Efficiencies & Comparisons

For experimental validation of the main EDN functionality, the prototype is controlled using the control structure proposed in [29]. The prototype is operated with a motion pattern identical to that of the moving floor application, with the highest motion cycle frequency, i.e. 16 cycles/minute. Under these motion conditions, 12 different load cases have been realized using different pressure reduction valve settings as specified in Table 2.

Table 2. Pressure reduction valve settings for the tests conducted. The pressure reduction valves have been adjusted manually and with the use of an analogue manometer for pressure monitoring.

Test #	Pressure reduction valve setting	Test #	Pressure reduction valve setting
1	All reduc. valves @ 0 [bar], orifices open	7	All reduction valves $\approx$ 100 [bar]
2	All reduction valves $\approx$ 10 [bar]	8	All reduction valves $\approx$ 120 [bar]
3	All reduction valves $\approx$ 15 [bar]	9	All reduction valves $\approx$ 140 [bar]
4	All reduction valves $\approx$ 40 [bar]	10	All reduction valves $\approx$ 160 [bar]
5	All reduction valves $\approx$ 60 [bar]	11	All reduction valves $\approx$ 180 [bar]
6	All reduction valves $\approx$ 80 [bar]	12	All reduction valves $\approx$ 200 [bar]

For detailed inspection, the relevant states of the testbench are depicted in Figure 2 for Test # 12. From Figure 2 (D), (E) and (F) it is evident that the piston positions tracks their references with a reasonable precision considering its industrial application, and the instantaneous lower chamber pressure is maintained in the vicinity of its pressure setting of 20 [bar]. Furthermore, it is notable that the piston pressure forces depicted in Figure 2 (B) do not settle at zero value even though the cylinders are horizontally mounted. The reason is that the control is subject to steady state position errors, causing the controller to provide a small input to the electric drives, and consequently, the pistons literally always move under these motion cycles, at least with a very low velocity . Therefore, the load actuator pistons also move, and the associated pressures, hence forces, are maintained at levels corresponding to the pressure reduction valve settings. When the cylinder pistons are controlled in the reverse direction, the pressure is relieved and the force reduced. However, the forces are not instantly increased in the reverse direction as the associated load actuator chambers need to be compressed before the reduction valve cracking pressures are reached. These properties comprise the main differences from the load in the industrial application.

Preprints.org (www.preprints.org) | NOT PEER-REVIEWED | Posted: 13 May 2024 doi:10.20944/preprints202405.0807.v1

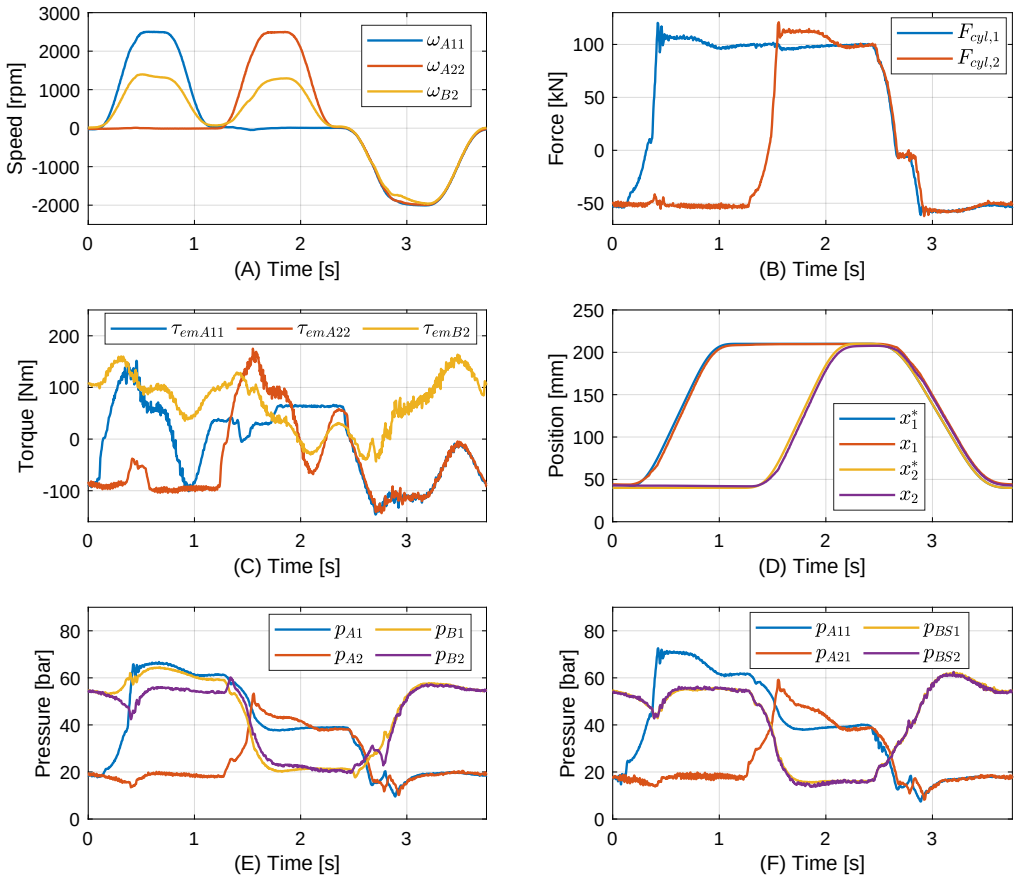

Figure 2. EDN states for Test # 12 operating at 16 motion cycles per minute. (A) Actual EM shaft speeds. (B) Hydraulic pressure forces of main cylinder pistons. (C) EM electro-magnetic torques. (D) Main cylinder piston positions and position commands (maked with superscript *). (E) Chamber pressures of main cylinders. (F) EDN side pressures.

Considering the electro-magnetic torques of the electric motors (EM's) in Figure 2 (C), these are subject to larger transients than the hydraulic pressure forces of the main cylinder pistons. The reason for this is the large acceleration torques required by the EMs compared to the necessary acceleration forces of the cylinder pistons. This is due to relatively large inertia of the combined rotary group of each VsD compared to the inertia mass of the cylinder/load actuator assemblies. Finally, the EM shaft speeds depicted in Figure 2 (A) appear well-behaved with the different maximum positive and negative speeds owed to the different main cylinder piston velocity requirements for piston extension and retraction.

The power at different points in the system during a single motion cycle for all 12 tests, are shown in Figure 3 along with the associated piston forces. First, it is found from the piston forces in Figure 3 (A) and (B), that the load actuator forces behaves similar to the description above in all tests. From Figure 3 (C) and (D) depicting the total power associated with the main cylinder pistons and the displacement unit outlets, these are found to have similar behavior. However, considering the total DC-bus power depicted in Figure 3 (E), the power associated with acceleration/deceleration of the EMs is clearly seen. Part of the power associated with deceleration of the EM shaft is passed towards the electric supply, and the energy intermediately stored in the supply capacitance.

 doi:10.20944/preprints202405.0807.v1

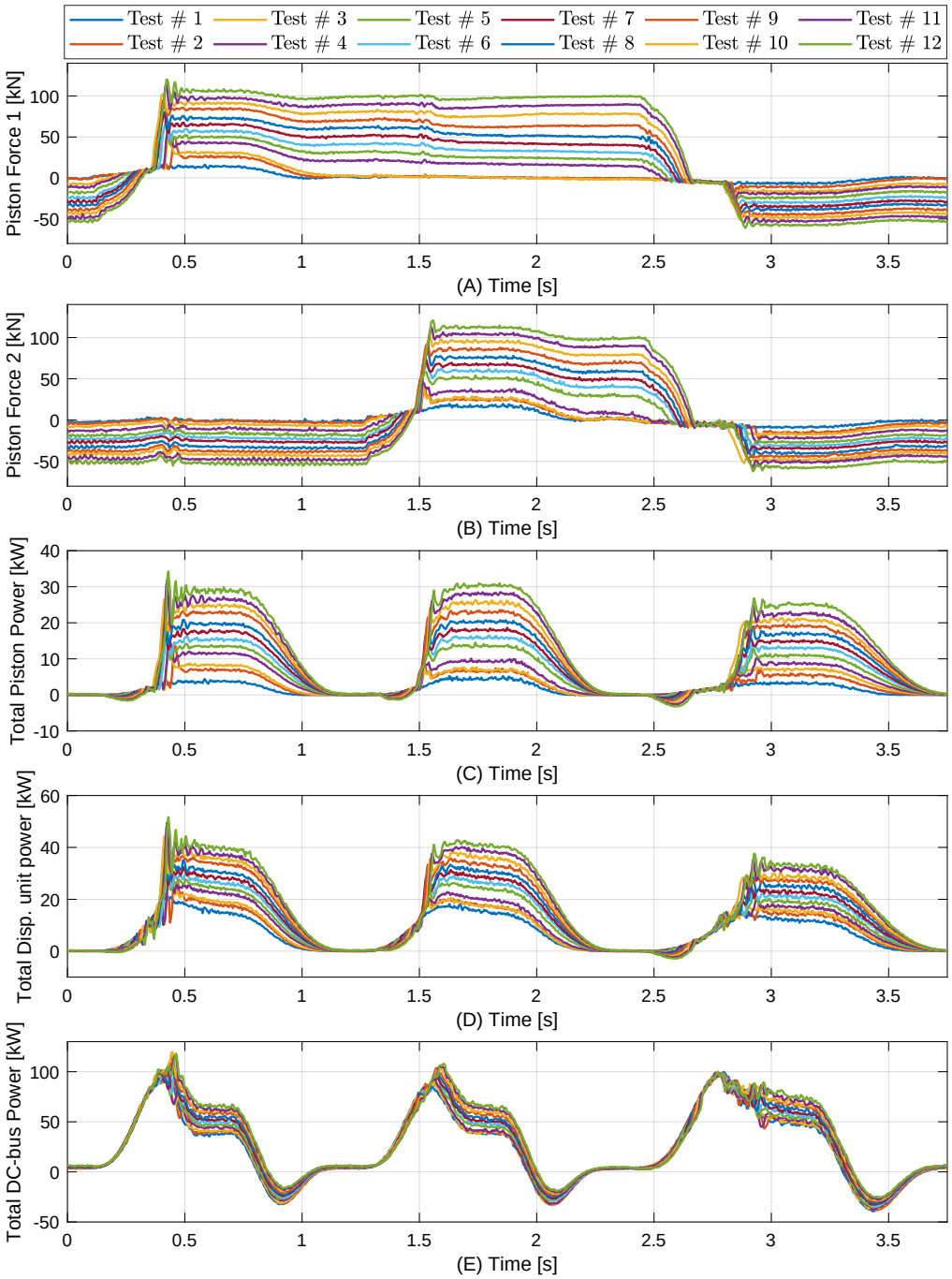

Figure 3. Force and power measures for all 12 EDN tests. (A) Hydraulic pressure forces of main cylinder 1. (B) Hydraulic pressure forces of main cylinder 2. (C) Total hydraulic output power of both cylinder 1 and cylinder 2. (D) Total displacement unit output power of all VsD's. (E) Total power of both electric supplies (DC-bus's).

Consider now specifically the hydraulic piston output power, the displacement unit output power and the DC-bus power of the electric supplies for Test # 12, depicted in Figure 4. Noting also the shaft speed example of Figure 2 (A), it is found that the DC-bus power associated with EM shaft acceleration is subject to a transient, approximately 65 % higher than the subsequent period of nearly constant speeds. However, as also found from Figure 4, the average DC-bus power is only approximately a third of the DC-bus peak power. The relatively large EM acceleration power level sets high requirements to the DC-bus peak power capacity, a feature that generally must be considered in detail for electro-hydraulic variable-speed drives to ensure that the intended performance is achievable.

 doi:10.20944/preprints202405.0807.v1

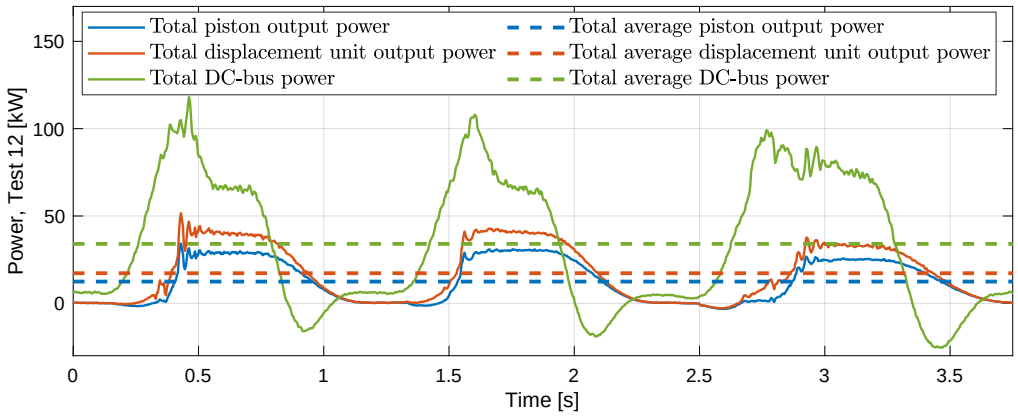

Figure 4. EDN power measures, including average levels, for Test # 12.

3.1. Comparison with Standalone Electro-Hydraulic Variable-Speed Drive System

Having considered the general performance features as well as the power characteristics of the EDN, it is relevant to consider its general properties and efficiencies when compared to standalone electro-hydraulic drive solution. The standalone electro-hydraulic drive (SED) solution considered here, is similar to those presented in e.g. [18], and is realized with the EDN testbench by closing the ball valve depicted in the schematics of Figure 1. This disables the short-circuit connection between the two cylinders, thereby removing the hydraulic coupling.

The main differences of the EDN and SED are associated with the supply unit functionality and whether the piston side chambers are short-circuited as for the EDN or not as for the SED. Considering the DU's these have to displace the same amount of fluid with respect to time and hence the associated flows for the EDN and SED closely resembles each other. However, for the EDN, SU1 and SU2 operate as a single unit connected to the common piston side volume, whereas for the SED the SU's are operated separately. Hence, the EDN supply unit function is realizable with less but larger components, potentially subject to less losses due to fewer transmission interfaces, and definitely less system integration effort.

The average efficiencies for the EDN and SED for the 12 test scenarios are calculated from the power measures and are depicted in Figure 5. From an efficiency point of view, the EDN and SED appear nearly identical. This is to be expected as the two drive system architectures are physically similar, contain the same components and perform the same output work.

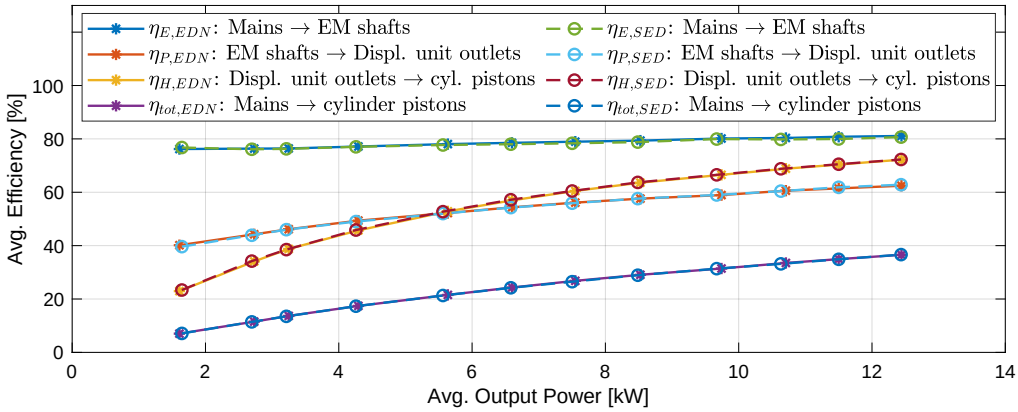

Figure 5. Average efficiency measures at different points in the EDN and SED, at 16 cycles/minute and all 12 load test cases.

3.1.1. Discussion

The efficiency measures appear rather low bearing in mind the absence of proportional control valves and hence conceptual losses. However, noting the pressure levels depicted in Figure 2, i.e. the

 doi:10.20944/preprints202405.0807.v1

test with the highest external load force, it may be clear that the drive systems and the actuators are only subject to minor loads. As an example, the bent axis hydraulic motors are designed for a nominal speed of 4000 [rpm] and a nominal pressure difference of 400 [bar], while the maximum shaft speed and pressure difference achieved in the tests are approximately 2510 [rpm] and 46 [bar], respectively. Hence, the bent axis hydraulic motors are indeed operated at part load with maximum speed and pressure difference being just 63 % and 12 % of their nominal ranges. For this reason the losses are relatively high compared to their outputs. Furthermore, the pressure losses in the pipes/hoses and fluid exchange mechanisms are mainly associated with the flows and hence the motion cycles. Therefore, as pressures are low, the associated losses are relatively high compared to the transmitted power. The expected efficiencies at higher loads are considered in the subsequent section.

3.2. *Efficiency Prediction at Increased External Loads*

In order to provide a prediction of the efficiency at higher load forces, models aided by experimental data are applied. Considering the losses of the pipe/hose/fluid exchange mechanisms, the modeling of these may be subject to substantial uncertainties, mainly due to the complexity of the logic cartridge valves used to realize the check functions. However, as the associated losses are mainly related to the flows and hence motion cycles, the measured losses are used while compensating for the effect of increased pressures. As reliable loss models for the used displacement units have not been available, the loss model of a fixed displacement axial piston motor presented in [27] is used as a basis. Here, the leakage levels are scaled according to the external leakage flows calculated from Eq. (1) for all the tests, as this measure accounts for all drain flows and other external leakages.

$$Q_{\Sigma\text{loss}} = D_\text{B}(\omega_{\text{B1}} + \omega_{\text{B2}}) - (A_\text{A} - A_\text{B})(\dot{x}_1 + \dot{x}_2) \tag{1}$$

Considering the electric system, no reliable loss model information has been available, and hence this is left out of the analysis. However, the combined efficiency of these components are expected to increase to above 90% when properly loaded.

In order to evaluate the efficiency at higher loads, models that scales the measured hydraulic forces are applied. The increased forces are generated using the measured pressure data for Test # 12. As the procedure is identical for both cylinders, only the process for cylinder 1 is presented here. Let p_{A1}, p_{B1} be the measured pressures associated with the measured pressure force $F_{\text{cyl1}} = A_\text{A} p_{\text{A1}} - A_\text{B} p_{\text{B1}}$, and let a scaled force be denoted $\hat{F}_{\text{cyl1}} = k_\text{s} F_{\text{cyl1}}$ where k_s is a scaling factor. Then the chamber pressures $\hat{p}_{\text{A1}}$, $\hat{p}_{\text{B1}}$ associated with the scaled force $\hat{F}_{\text{cyl1}}$, may be calculated by Eqs. (2) and (3).

$$\hat{p}_{\text{A1}} = \begin{cases} \dfrac{A_\text{B} p_{\text{B1}} + \hat{F}_{\text{cyl1}}}{A_\text{A}} & \text{for} \quad \hat{F}_{\text{cyl1}} \geq (A_\text{A} - A_\text{B})\min(p_{\text{A1}}, p_{\text{B1}}) \\ \min(p_{\text{A1}}, p_{\text{B1}}) & \text{for} \quad \hat{F}_{\text{cyl1}} < (A_\text{A} - A_\text{B})\min(p_{\text{A1}}, p_{\text{B1}}) \end{cases} \tag{2}$$

$$\hat{p}_{\text{B1}} = \begin{cases} \min(p_{\text{A1}}, p_{\text{B1}}) & \text{for} \quad \hat{F}_{\text{cyl1}} \geq (A_\text{A} - A_\text{B})\min(p_{\text{A1}}, p_{\text{B1}}) \\ \dfrac{A_\text{A} p_{\text{A1}} - \hat{F}_{\text{cyl1}}}{A_\text{B}} & \text{for} \quad \hat{F}_{\text{cyl1}} < (A_\text{A} - A_\text{B})\min(p_{\text{A1}}, p_{\text{B1}}) \end{cases} \tag{3}$$

Hence, the scaled force $\hat{F}_{\text{cyl1}}$ has the same *shape* as the measured force used, and the instantaneous lower pressure is identical to the corresponding measured pressure.

The predicted efficiencies are shown in Figure 6, demonstrating that the predicted and measured efficiencies closely resemble each other in the lower output power range. The main discrepancies between the measured and simulated efficiencies are related to the predicted displacement unit efficiencies, which slightly deviate at the lower output power levels. However, the main interest is the predicted efficiency from EM shaft to cylinder pistons depicted in Figure 6, suggesting a maximum efficiency for the considered motion cycle of approximately 77% from EM shafts to cylinder pistons at an average output power of 110 [kW]. The industrial moving floor application is, for the considered

Preprints.org (www.preprints.org) | NOT PEER-REVIEWED | Posted: 13 May 2024 doi:10.20944/preprints202405.0807.v1

motion cycle, expected to have an average output power of 80 [kW], and hence a predicted efficiency from EM shafts to cylinder pistons of approximately 76%. Assuming a total average electric system efficiency of 90% under this load, the total average system efficiency from electric supplies to cylinder pistons is expected to be approximately 68%.

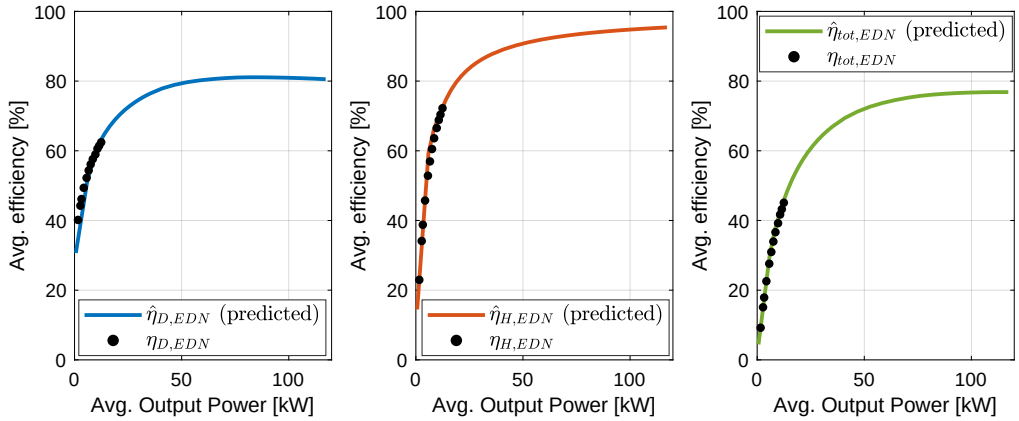

Figure 6. Predicted efficiencies for specified motion cycles and increased loads, and comparison with tests. (A) Total efficiency of all displacement units. (B) Total efficiency of all pipes/hoses/fluid exchange mechanisms. (C) Total efficiency from EM shafts to the main cylinder pistons.

3.3. Comparison with Valve Drive System Solution

Having compared the EDN to the SED, it is relevant also to compare the EDN to a conventional valve drive system solution. In the following a drive system controlled by 4/3 proportional control valves fed by a variable-speed pump is denoted a *valve drive system* (VDS), with such a system depicted in Figure 7.

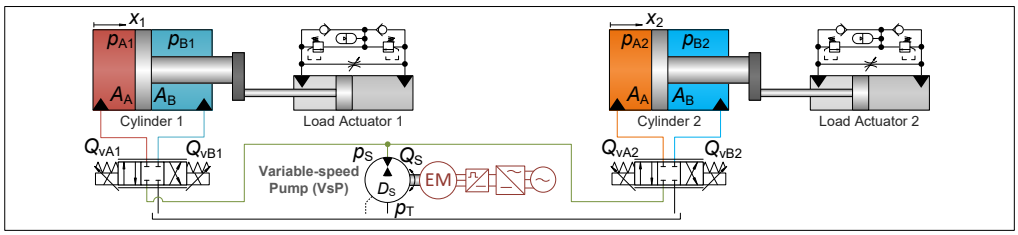

Figure 7. Schematics of proportional valve drive system fed by variable-speed pump (VDS).

To evaluate the power needed to provide the same work as the EDN, consider now the port flows for the valve associated with cylinder 1 given by Eqs. (4) and (5) for positive and negative piston motion, respectively. Here, x_{v1} is the associated spool position, k_v the valve flow gain and σ the ratio of the valve port flow gains.

$$Q_{vA1} = k_v x_{v1}\sqrt{p_S - p_{A1}}\ ,\quad Q_{vB1} = \sigma k_v x_{v1}\sqrt{p_{B1} - p_T}\quad \text{for}\quad \dot{x}_1 > 0 \tag{4}$$

$$Q_{vA1} = k_v x_{v1}\sqrt{p_{A1} - p_T}\ ,\quad Q_{vB1} = \sigma k_v x_{v1}\sqrt{p_S - p_{B1}}\quad \text{for}\quad \dot{x}_1 < 0 \tag{5}$$

Under steady state conditions and leakages absent at positive piston motion ($\dot{x}_1 > 0$), the flows Q_{vA1}, Q_{vB1} are related according to Eq. (6) where $A_B = \alpha A_B$.

$$\begin{aligned} \alpha Q_{vA1} = Q_{vB1} \quad &\Rightarrow \quad \alpha k_v x_{v1}\sqrt{p_S - p_{A1}} = \sigma k_v x_{v1}\sqrt{p_{B1} - p_T} \\ &\Rightarrow \quad \alpha^2(p_S - p_{A1}) = \sigma^2(p_{B1} - p_T) \end{aligned} \tag{6}$$

Indeed, for $\dot{x}_1 > 0$ the supply pressure must satisfy $p_S > p_{A1}$. This condition may be expressed as $p_S = p_\Delta + p_{A1}$ where p_Δ is some pressure margin necessary for the valve to realize the required flow.

 doi:10.20944/preprints202405.0807.v1

Using this, and the fact that $F_{\text{cyl1}} = A_{\text{A}} p_{\text{A1}} - A_{\text{B}} p_{\text{B1}}$, then from Eq. (6) the supply pressure is obtained as Eq. (7). Similarly, for $\dot{x}_1 < 0$, the supply pressure is given by Eq. (8).

$$p_{\text{S}}|_{\dot{x}_1>0} = p_{\text{S}} = \frac{\alpha^3 + \sigma^2}{\sigma^2} p_\Delta + \alpha p_{\text{T}} + \frac{F_{\text{cyl1}}}{A_{\text{A}}} \quad \text{for} \quad \dot{x}_1 > 0 \tag{7}$$

$$p_{\text{S}}|_{\dot{x}_1<0} = p_{\text{S}} = \frac{\alpha^3 + \sigma^2}{\alpha^3} p_\Delta + \frac{p_{\text{T}}}{\alpha} + \frac{F_{\text{cyl1}}}{\alpha A_{\text{A}}} \quad \text{for} \quad \dot{x}_1 < 0 \tag{8}$$

Using a similar approach for cylinder 2 and its associated valve, the supply pressures appear as Eqs. (9), (10).

$$p_{\text{S}}|_{\dot{x}_2>0} = p_{\text{S}} = \frac{\alpha^3 + \sigma^2}{\sigma^2} p_\Delta + \alpha p_{\text{T}} + \frac{F_{\text{cyl2}}}{A_{\text{A}}} \quad \text{for} \quad \dot{x}_2 > 0 \tag{9}$$

$$p_{\text{S}}|_{\dot{x}_2<0} = p_{\text{S}} = \frac{\alpha^3 + \sigma^2}{\alpha^3} p_\Delta + \frac{p_{\text{T}}}{\alpha} + \frac{F_{\text{cyl2}}}{\alpha A_{\text{A}}} \quad \text{for} \quad \dot{x}_2 < 0 \tag{10}$$

Hence, for a load sensing control function emulating that of conventional hydraulic power units, the necessary supply pressure may be estimated as Eq. (11).

$$\hat{p}_{\text{S}} = \max(p_{\text{S}}|_{\dot{x}_1>0}, p_{\text{S}}|_{\dot{x}_1<0}, p_{\text{S}}|_{\dot{x}_2>0}, p_{\text{S}}|_{\dot{x}_2<0}) \tag{11}$$

The pump flow is estimated as Eq. (12) and hence the pump outlet power is estimated as Eq. (13).

$$\hat{Q}_{\text{S}} = \hat{Q}_{\text{S1}} + \hat{Q}_{\text{S2}} \tag{12}$$

$$\hat{Q}_{\text{S1}} = \begin{cases} A_{\text{A}} \dot{x}_1 & \text{for} \quad \dot{x}_1 \geq 0 \\ -A_{\text{B}} \dot{x}_1 & \text{for} \quad \dot{x}_1 < 0 \end{cases}, \quad \hat{Q}_{\text{S2}} = \begin{cases} A_{\text{A}} \dot{x}_2 & \text{for} \quad \dot{x}_2 \geq 0 \\ -A_{\text{B}} \dot{x}_2 & \text{for} \quad \dot{x}_2 < 0 \end{cases}$$

$$\hat{P}_{\text{S}} = \hat{p}_{\text{S}} \hat{Q}_{\text{S}} \tag{13}$$

Using the above, as well as the displacement unit loss model used in the previous section, $p_\Delta = 10$ [bar], and assuming an efficiency of the electric system of 80% similar to the EDN measurements in Figure 5, the estimated efficiencies for the VDS compared to the EDN are depicted in Figure 8 for all 12 test cases. Here, both the case of using symmetric valves ($\sigma = 1$) and using matched valves ($\sigma = \alpha$), are presented.

Evidently, the efficiencies of the VDS's are lower than those of the EDN. In fact for e.g., Test # 12, the total EDN efficiency is 22 % and 66 % higher than the efficiencies of the matched and symmetric VDS's, respectively.

Predicting the expected efficiencies similarly to the previous section, the results appear as depicted in Figure 9. It is found that the total VDS efficiencies never exceeds 55% in any case for this system with the specified motion cycle, even when hose losses are neglected as considered here. Furthermore, it is notable that the EDN improves the system efficiency by ≈40 % and ≈47 % compared to the VDS's with matched and symmetric valves, respectively.

Preprints.org (www.preprints.org) | NOT PEER-REVIEWED | Posted: 13 May 2024 doi:10.20944/preprints202405.0807.v1

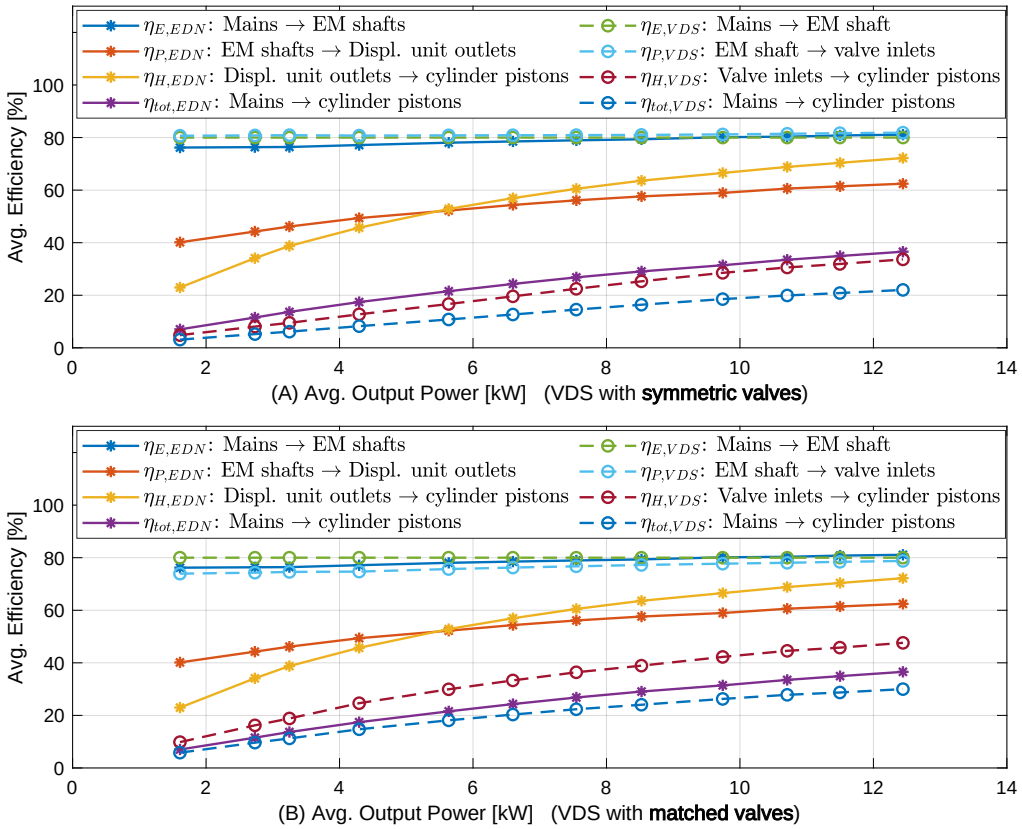

Figure 8. Measured average EDN efficiency measures, and VDS efficiency measures estimated from measured cylinder pressures and flows. (A) The EDN and VDS with symmetric valve spools. (B) The EDN and VDS with valve spools matched to the cylinder area ratios.

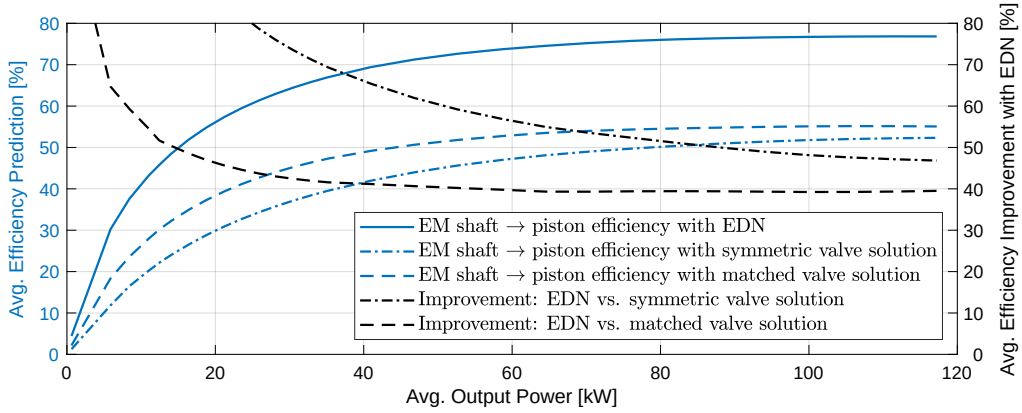

Figure 9. Predicted EM shaft-to-piston efficiencies with EDN and VDS solutions with symmetric and matched valves, and improvements with EDN compared to VDS's.

3.3.1. Discussion

The presented results are associated with the use of 4/3 valves in general and not any specific valves. This emphasizes the crucial importance of not only using variable-speed pumps in the endeavors to improve hydraulic system efficiencies, but to develop system architectures that do not rely on control valves in order to realize efficient hydraulic systems.

4. Conclusion

The first experimental results for electro-hydraulic variable-speed drive network technology are presented. This technology field has only recently been introduced, and developments presented in

 doi:10.20944/preprints202405.0807.v1

literature have so far been of theoretical nature, focusing on its key properties in terms of system control, downsizing capabilities, system design foundations as well as application to a crane and a construction machine. In this article the first electro-hydraulic variable-speed drive network prototype ever build is presented. The prototype has been developed for a so-called moving floor application allowing demonstration in an industrial environment, and comprises two identical cylinders to be controlled. The electro-hydraulic variable-speed drive network prototype is realized with short-circuit of the rod side cylinder chambers, and comprises three electric motor/displacement unit functions. However, due to large cylinder diameters and high motion cycle frequency requirements, the resulting flows are rather large, and due to the available component sizes, the prototype is realized with paired electric motors/displacement units in order to meet the flow requirements. Furthermore, as a consequence of the large cylinder diameters, only part loads are realizable by the load actuators under laboratory conditions. Experimental data has been acquired while conducting motion cycle associated with the industrial application, under twelve different load cases, and the results are presented, demonstrating feasible performance in terms of motion and pressure control. Furthermore, as only part load tests have been realizable, data-aided models have been used to predict the total efficiency under higher loads. Results predict a total average efficiency from the electric supply to the cylinder pistons of 68%. Also, the experimental results from the electro-hydraulic variable-speed drive network prototype has been compared to those of a standalone electro-hydraulic drive system, showing similar efficiencies. Finally, the electro-hydraulic variable-speed drive network prototype is compared to a conventional valve drive solution, implying that a maximum efficiency under the considered load cycles of 55% is achievable with a valve solution. To this end, electro-hydraulic variable-speed drive network prototype is found to provide efficiency improvements of at least 40% in comparison to a valve solution.

Author Contributions: Conceptualization, L.S.; methodology, L.S., M.B.G.; formal analysis, L.S., M.B.G.; investigation, L.S., M.B.G.; writing-original draft preparation, L.S.; writing-review and editing, L.S., M.B.G.; visualization, L.S.; project administration, L.S.; funding acquisition, L.S. Both authors have read and agreed to the published version of the manuscript.

Funding: This research was funded by the Danish Energy Agency, the Energy Technology Development and Demonstration Programme, project: *Efficient Cement Handling Systems Based on Electro-Hydraulic Power Regeneration Networks* (eCHASPOR), project number 64020-2046.

Conflicts of Interest: The authors declare no conflict of interest.

Abbreviations

The following abbreviations are used in this manuscript:

EDN	Electro-hydraulic variable-speed drive network
EM	Electric motor
SED	Standalone electro-hydraulic variable-speed drive system
VDS	Valve drive system fed by electro-hydraulic variable-speed pump
VsD	Variable-speed displacement unit

References

1. Scheidl, R.; Gradl, C.; Kogler, H.; Foschum, P.; Plöckinger, A. Investigation of a Switch-Off Time Variation Problem of a Fast Switching Valve. ASME/BATH 2014 Symposium on Fluid Power and Motion Control, FPMC 2014. American Society of Mechanical Engineers Digital Collection, 2014. doi:10.1115/FPMC2014-7851.
2. Kogler, H.; Scheidl, R.; Schmidt, B.H. Analysis of Wave Propagation Effects in Transmission Lines due to Digital Valve Switching. ASME/BATH 2015 Symposium on Fluid Power and Motion Control, FPMC 2015. American Society of Mechanical Engineers Digital Collection, 2016. doi:10.1115/FPMC2015-9607.
3. Huova, M.; Linjama, M.; Siivonen, L.; Deubel, T.; Försterling, H.; Stamm, E. Novel Fine Positioning Method for Hydraulic Drives Utilizing On/Off-Valves. BATH/ASME 2018 Symposium on Fluid Power and Motion Control, FPMC 2018. American Society of Mechanical Engineers Digital Collection, 2018. doi:10.1115/FPMC2018-8891.

4. Midgley, W.J.; Abrahams, D.; Garner, C.P.; Caldwell, N. Modelling and experimental validation of the performance of a digital displacement® hydraulic hybrid truck:. *Proceedings of the Institution of Mechanical Engineers* **2021**. doi:10.1177/09544070211026196.
5. Rampen, W.; Dumnov, D.; Taylor, J.; Dodson, H.; Hutcheson, J.; Caldwell, N. A Digital Displacement Hydrostatic Wind-turbine Transmission. *International Journal of Fluid Power* **2021**, *21*, 87–112–87–112. doi:10.13052/IJFP1439-9776.2213.
6. MacPherson, J.; Williamson, C.; Green, M.; Caldwell, N. Energy efficient excavator hydraulic systems with digital displacement® pump-motors and digital flow distribution. BATH/ASME 2020 Symposium on Fluid Power and Motion Control, FPMC 2020. American Society of Mechanical Engineers Digital Collection, 2020. doi:10.1115/FPMC2020-2770.
7. Hutcheson, J.; Abrahams, D.; MacPherson, J.; Caldwell, N.; Rampen, W. Demonstration of efficient energy recovery systems using digital displacement® hydraulics. BATH/ASME 2020 Symposium on Fluid Power and Motion Control, FPMC 2020. American Society of Mechanical Engineers Digital Collection, 2020. doi:10.1115/FPMC2020-2767.
8. Budden, J.J.; Williamson, C. Danfoss Digital Displacement® Excavator: Test results and analysis. ASME/BATH 2019 Symposium on Fluid Power and Motion Control, FPMC 2019. American Society of Mechanical Engineers Digital Collection, 2020. doi:10.1115/FPMC2019-1669.
9. Hansen, A.H.; Asmussen, M.F.; Bech, M.M. Hardware-in-the-loop Validation of Model Predictive Control of a Discrete Fluid Power Take-Off System for Wave Energy Converters. *Energies* **2019**, *12*, 3668. doi:10.3390/en12193668.
10. Hansen, A.H.; Asmussen, M.F.; Bech, M.M. Model Predictive Control of a Wave Energy Converter with Discrete Fluid Power Take-Off System. *Energies* **2018**, *11*, 635. doi:10.3390/en11030635.
11. Zagar, P.; Kogler, H.; Scheidl, R.; Winkler, B. Hydraulic Switching Control Supplementing Speed Variable Hydraulic Drives. *Actuators 2020, Vol. 9, Page 129* **2020**, *9*, 129. doi:10.3390/ACT9040129.
12. Johansen, P.; Hansen, A.H. A Digital Hydraulic Full-Bridge Oscillation Transformer. ASME/Bath 2023 Symposium on Fluid Power and Motion Control. American Society of Mechanical Engineers Digital Collection, 2023. doi:10.1115/FPMC2023-111865.
13. Michel, S.; Weber, J. Energy-efficient electrohydraulic compact drives for low power applications. BATH 2012 Symposium on Fluid Power and Motion Control, FPMC 2012, 2012.
14. Wiens, T.; Deibert, B. A low-cost miniature electrohydrostatic actuator system. *Actuators* **2020**, *9*, 1–16. doi:10.3390/act9040130.
15. Stawinski, L.; Skowronska, J.; Kosucki, A. Energy Efficiency and Limitations of the Methods of Controlling the Hydraulic Cylinder Piston Rod under Various Load Conditions. *Energies 2021, Vol. 14, Page 7973* **2021**, *14*, 7973. doi:10.3390/EN14237973.
16. Zhang, S.; Li, S.; Minav, T. Control and Performance Analysis of Variable Speed Pump-Controlled Asymmetric Cylinder Systems under Four-Quadrant Operation. *Actuators* **2020**, *9*, 123. doi:10.3390/act9040123.
17. Casoli, P.; Scolari, F.; Minav, T.; Rundo, M. Comparative energy analysis of a load sensing system and a zonal hydraulics for a 9-tonne excavator. *Actuators* **2020**, *9*, 39. doi:10.3390/ACT9020039.
18. Helduser, S. Hydraulische Antriebssysteme mit drehzahlverstellbarer pumpe. *Ölhydraulik und Pneumatik* **1997**, *41*.
19. Kärnell, S.; Ericson, L. Control of an Asymmetric Cylinder With Two Individually Controlled Pump/Motors. ASME/Bath 2023 Symposium on Fluid Power and Motion Control. American Society of Mechanical Engineers Digital Collection, 2023. doi:10.1115/FPMC2023-109710.
20. Qu, S.; Fassbender, D.; Vacca, A.; Busquets, E. A high-efficient solution for electro-hydraulic actuators with energy regeneration capability. *Energy* **2021**, *216*, 119291. doi:10.1016/j.energy.2020.119291.
21. Padovani, D. Leveraging Flow Regeneration in Individual Energy-Efficient Hydraulic Drives. ASME/BATH 2021 Symposium on Fluid Power and Motion Control, FPMC 2021. American Society of Mechanical Engineers Digital Collection, 2021.
22. Qu, S.; Zappaterra, F.; Vacca, A.; Busquets, E. An electrified boom actuation system with energy regeneration capability driven by a novel electro-hydraulic unit. *Energy Conversion and Management* **2023**, *293*, 117443. doi:https://doi.org/10.1016/j.enconman.2023.117443.

23. Fassbender, D.; Minav, T.; Brach, C.; Huhtala, K. Improving the Energy Efficiency of Single Actuators with High Energy Consumption: An Electro-Hydraulic Extension of Conventional Multi-Actuator Load-Sensing Systems. Scandinavian International Conference on Fluid Power, 2021, pp. 74–89.
24. Siefert, J.; Li, P.Y. Optimal Control of the Energy-Saving Hybrid Hydraulic-Electric Architecture (HHEA) for Off-Highway Mobile Machines. *IEEE Transactions on Control Systems Technology* **2022**, *30*, 2018–2029. doi:10.1109/TCST.2021.3131435.
25. Wills, J.; Li, P.Y. Electric and Hydraulic Propel Torque Modulation for a Compact Track Loader With the Hybrid Hydraulic Electric Architecture (HHEA). ASME/Bath 2023 Symposium on Fluid Power and Motion Control. American Society of Mechanical Engineers Digital Collection, 2023. doi:10.1115/FPMC2023-112035.
26. Chatterjee, A.; Li, P.Y. Human-in-the-Loop Motion Control of a Two-DOF Hydraulic Backhoe Powered by the Hybrid Hydraulic Electric Architecture (HHEA). ASME/Bath 2023 Symposium on Fluid Power and Motion Control. American Society of Mechanical Engineers Digital Collection, 2023. doi:10.1115/FPMC2023-111819.
27. Schmidt, L.; Hansen, K.V. Electro-Hydraulic Variable-Speed Drive Networks—Idea, Perspectives, and Energy Saving Potentials. *Energies* **2022**, *15*, 1228. doi:10.3390/en15031228.
28. Schmidt, L.; Ketelsen, S.; Hansen, K.V. Perspectives on Component Downsizing in Electro-Hydraulic Variable-Speed Drive Networks. Bath/ASME 2022 Symposium on Fluid Power and Motion Control, FPMC 2022. American Society of Mechanical Engineers Digital Collection, 2022. doi:10.1115/FPMC2022-89547.
29. Schmidt, L.; Ketelsen, S.; Hansen, K.V. State Decoupling and Stability Considerations in Electro-Hydraulic Variable-Speed Drive Networks. Bath/ASME 2022 Symposium on Fluid Power and Motion Control, FPMC 2022. American Society of Mechanical Engineers Digital Collection, 2022. doi:10.1115/FPMC2022-89548.
30. van Binsbergen-Galán, M.; Schmidt, L. Determination of Load Collective for Sizing of a Hydraulic Drive Network System Considering Simultaneity Between Actuator Loads. ASME/Bath 2023 Symposium on Fluid Power and Motion Control. American Society of Mechanical Engineers Digital Collection, 2023. doi:10.1115/FPMC2023-109823.
31. Schmidt, L.; van Binsbergen-Galán, M.; Knöll, R.; Riedmann, M.; Schneider, B.; Heemskerk, E. Energy Efficient Excavator Functions Based on Electro-Hydraulic Variable-Speed Drive Network. 14. International Fluid Power Kolloquium (IFK), 2024.